# Thermodynamic Assessment of the $CaO–Al_2O_3–SiO_2$ System

Huahai Mao,† Mats Hillert, Malin Selleby, and Bo Sundman

Department of Materials Science and Engineering, Division of Computational Thermodynamics, KTH (Royal Institute of Technology), SE-100 44 Stockholm, Sweden

**The $CaO–Al_2O_3–SiO_2$ system has been assessed with the CALPHAD technique, based on recent assessments of its binary systems. A new species $AlO_2^{-1}$ was introduced for modeling liquid $Al_2O_3$. The ternary liquid phase was described using the ionic two-sublattice model as $(Al^{+3}, Ca^{+2})_P$ $(AlO_2^{-1}, O^{-2}, SiO_4^{-4}, SiO_2^0)_Q$. The available experimental data were critically examined, and a self-consistent set of thermodynamic descriptions was obtained. Various phase diagrams and property diagrams, including isothermal sections, isoactivity lines, and a projection of the liquidus surface, are presented. Information on viscosity seems to support the use of the $AlO_2^{-1}$ species.**

## I. Introduction

THE thermodynamic description of the ternary $CaO–Al_2O_3–SiO_2$ system must be based on the assessment of the three binaries, and it is necessary that they are described with compatible models, especially for the liquid phase. The ionic two-sublattice liquid model[1,2] and the quasi-chemical modification of the substitutional model[3] are designed for this purpose.

With the quasi-chemical approach,[4] the model is described with the formula ($CaO$, $SiO_2$) in the $CaO–SiO_2$ system, and a short-range order is considered by interaction of bonds between second-nearest neighbors Ca and Si, i.e. one Ca–Ca pair separated by a free oxygen and one Si–Si pair joined by a bridging oxygen forming two Ca–Si pairs separated by broken oxygen bridges. With the two-sublattice model,[5,6] the liquid was described with the formula $(Ca^{+2})_P(O^{-2}, SiO_4^{-4}, SiO_2^0)_Q$ where the $SiO_2^0$ species represents the tetrahedral network of pure liquid silica, and the mixture of the $SiO_4^{-4}$ and $SiO_2^0$ species represents the variable degree of polymerization for compositions between $Ca_2SiO_4$ and $SiO_2$. The liquid in the $Al_2O_3–SiO_2$ system was first modeled by Kaufman[7] as an ordinary substitutional solution using the formula ($Al_{0.4}O_{0.6}$, $Si_{0.33}O_{0.67}$) and then by Dörner *et al.*[8] and Howald and Eliezer[9] using ($AlO_{1.5}$, $SiO_2$). The latter formula actually describes the mixtures of Al and Si atoms in an O atmosphere. This model was accepted by Eriksson and Pelton,[10] but it was modified by the introduction of a quasi-chemical ordering effect. Using the ionic two-sublattice model, Hillert *et al.*[11] applied the formula $(Al^{+3})_P(O^{-2}, SiO_4^{-4}, SiO_2^0)_Q$. For the $CaO–Al_2O_3$ system, Eriksson and Pelton[10] applied the formula ($CaO$, $AlO_{1.5}$) and Hallstedt[12] applied the formula $(Al^{+3}, Ca^{+2})_P(O^{-2})_Q$. There were thus two sets of compatible binary descriptions that could be used for the ternary $CaO–Al_2O_3–SiO_2$ system. Eriksson and Pelton[10] were able to provide a successful description using the formula ($CaO$, $AlO_{1.5}$, $SiO_2$). However, when Wang *et al.*[13] applied the ionic two-sublattice model using the formula $(Al^{+3}, Ca^{+2})_P(O^{-2}, SiO_4^{-4}, SiO_2^0)_Q$ they encountered some difficulties. A miscibility gap appeared in the $(Al^{+3}, Ca^{+2})_P(O^{-2}, SiO_4^{-4})_Q$ subsystem, which was difficult to suppress even with a so-called reciprocal parameter $L_{Al^{+3}, Ca^{+2}:O^{-2}, SiO_4^{-4}}$. Furthermore, it was not possible to make the liquid miscibility gap, originating from the $SiO_2$-rich part of the $CaO–SiO_2$ binary side, sufficiently narrow.

In addition to the two basic models, the quasi-chemical model and the two-sublattice model, many other models have been proposed for determination of the thermodynamic properties of slags in the $CaO–Al_2O_3–SiO_2$ system. One can mention the following ones: the cellular model by Kapoor and Frohberg,[14] later extended by Gaye and Welfringer,[15] the associate solution models by Larrain and Kellogg,[16] Hastie *et al.*,[17] and Björkman,[18] the polynomial representation of liquid complexes by Hoch,[19] and, finally, the stoichiometric–Margules solution model by Berman and Brown.[20] Most of the models can reproduce binary phase diagrams rather well, but their ability to predict multicomponent properties from the binary systems is usually rather limited.

In the present work, an attempt will be made to modify the ionic two-sublattice liquid model to provide a better description of the $CaO–Al_2O_3–SiO_2$ system.

## II. Modification of the Ionic Two-Sublattice Model

The liquid miscibility gap in the $SiO_2$-rich part of the $CaO–SiO_2$ system is a common feature of several binary $MO–SiO_2$ systems with basic MO oxides, and it disappears quickly when $Al_2O_3$ is added. In previous attempts to assess the $CaO–Al_2O_3–SiO_2$ system with the ionic two-sublattice liquid model, this miscibility gap on the $CaO–SiO_2$ side extended too far into the ternary system.[13] Attempts to avoid this in the present work by using various ternary parameters failed. It thus seemed that the difficulty may be related to the modeling of $Al_2O_3$. Before considering this question, one should consider how liquid $SiO_2$ is modeled. It can then be realized that the neutral species, $SiO_2^0$, was used in order to mimic the large network in pure silica where Si has a coordination number of CN = 4 and is tetrahedrally surrounded by four O atoms. Each O forms a bridge between two Si atoms. The network breaks up gradually with the addition of oxygen through a basic oxide like CaO, and finally all the Si atoms appear as $SiO_4^{-4}$ ions, where Si is still tetrahedrally surrounded by four O. By introducing the $SiO_4^{-4}$ species in the same sublattice as $SiO_2^0$, it was possible to mimic the thermodynamic effect of the gradual formation of smaller fragments from the silica network when a basic oxide like CaO is added.[1–3]

From crystallized silicates, it is known that Al can form covalently bonded $AlO_4$ tetrahedra, which may share all four corners and are very similar to the $SiO_4$ tetrahedra, and it has been regarded as reasonable to expect the same in alumino-silicate melts.[21–27] However, in pure $Al_2O_3$, there are very few oxygen atoms aiding the formation of a tetrahedral network but O atoms can be incorporated by the addition of a basic oxide. Already, Kozakevitch[22] pointed out that in the $SiO_2–CaAl_2O_4$ section, the amount of CaO is exactly the correct value that leads to the possibility for all the Al atoms to form such tetrahedra and to merge with $SiO_4$ tetrahedra into a large network. In recent years, new experimental techniques have yielded some support for this proposal. Even though the stoichiometry of

$Al_2O_3$ suggests CN = 3, studies with molecular dynamic simulations[24–26] and Al nuclear magnetic resonance measurements[27] indicate that CN = 4 predominates. In particular, Benoit and Ispas[26] compared the structural properties between molten $CaO–Al_2O_3–SiO_2$ and $SiO_2$ in their recent molecular dynamic simulations. They found that the first addition of CaO to liquid $Al_2O_3–SiO_2$ would not break the O bridges between metal atoms of CN = 4 but would further increase the predominance of CN = 4 for the Al atoms. For compositions in the $CaAl_2O_4–SiO_2$ section, it would thus be possible, at least in principle, to have exactly the same network as in pure $SiO_2$. It would seem possible to model this network as a mixture of the two species $SiO_2^0$ and $AlO_2^{-1}$. The $Ca^{+2}$ ions would be dissolved interstitially within this network.

When the O bridges in $SiO_2$ are broken by the new O atoms supplied by the addition of a basic oxide, the oxygen of a broken bridge will have a negative charge, compensating the charge of the cation. On the other hand, the negative charge of $AlO_2^{-1}$ may rather be connected to the centrally situated Al atom in the O tetrahedron because all those O atoms form bridges.

Some important questions should now be considered.

(1) On the CaO side of the $SiO_2–CaO \cdot Al_2O_3$ join, will the additional O atoms start to break bridges, as they do in the $CaO–SiO_2$ system, and finally form $AlO_4^{-5}$ ions, similar to the $SiO_4^{-4}$ ions?

(2) If so, will those $AlO_4^{-5}$ ions be stable all the way to small amounts of $Al_2O_3$, just as the $SiO_4^{-4}$ ions are supposed to be stable close to the CaO corner, or will they dissociate into $Al^{+3}$ and $O^{-2}$ ions?

(3) Can Al be incorporated into the $SiO_2$ network already in the $SiO_2–Al_2O_3$ system before the addition of a basic oxide, and how will the Al–O associates in pure $Al_2O_3$ look?

There seems to be no direct information that can help to answer these questions but considering the amphoteric character of $Al_2O_3$, it seems that at least some $Al^{+3}$ cations should always form by dissociation of $Al_2O_3$. The corresponding O atoms could be present as $O^{-2}$ ions but some of them could associate with other Al atoms. In addition to the 1.5 O atoms per Al in $Al_2O_3$, these extra O atoms, formed by dissociation, can help to build larger and larger associates, if the amount of $Al_2O_3$ is increased, until a complete network is formed, similar to the network in $SiO_2$. If such a network occurs in pure $Al_2O_3$, that compound should be modeled with the formula $(Al^{+3})_1(AlO_2^{-1})_3$ where a quarter of the aluminum oxide acts as a basic oxide. It should be emphasized that this model would yield no entropy of mixing to pure $Al_2O_3$ because the two species are present in different sublattices. An important question would be: how will the fraction of the Al atoms, which form $Al^{+3}$ ions, vary through the $CaO–Al_2O_3$ system? Since the present work should be regarded only as the first attempt to formulate such a model, no particular parameter will be introduced to affect this fraction.

In the $CaO–SiO_2$ system, the gradual fragmentation of the $SiO_2$ network, which finally leads to the formation of $SiO_4^{-4}$ ions, was modeled by a mixture of $SiO_2^0$ and $SiO_4^{-4}$. In a similar fashion, the gradual fragmentation of the $AlO_2^{-1}$ network, including dissociation into simple ions, will be modeled by a mixture of $AlO_2^{-1}$ and $Al^{+3}$. The $CaO–Al_2O_3$ system will thus be modeled as $(Al^{+3}, Ca^{+2})_P(AlO_2^{-1}, O^{-2})_Q$, and the $AlO_4^{-5}$ species will not be introduced. In the $CaO–SiO_2$ system, there is a strong thermodynamic effect at the composition $2CaO \cdot SiO_2$ where all the Si atoms in principle can form $SiO_4^{-4}$ ions, indicating that most of them do. In the $CaO–Al_2O_3$ system, there is no similar effect at the $5CaO \cdot 2Al_2O_3$ composition, which indicates that the $AlO_4^{-5}$ associates are less stable, which provides a justification for not including that kind of species in the formula.

The liquid phase in the $SiO_2–Al_2O_3$ system has often been modeled as a mixture of Si and Al in an atmosphere of O using the substitutional model ($SiO_2$, $AlO_{1.5}$). It has been applied with reasonable success in assessments of the phase diagram and thermodynamic properties.[10] However, it seems to build on the assumption that the Al atoms in the network are surrounded by only three O atoms, which is contrary to theoretical expectations. The present work will instead be based on the description of pure $Al_2O_3$ just given for the $CaO–Al_2O_3$ system, which yields the model $(Al^{+3})_P(AlO_2^{-1}, SiO_2^0)_Q$. Thanks to the presence of $Al^{+3}$, the first addition of CaO will not lead to bridge breakage. The new O atoms may instead react with $Al^{+3}$ to form more $AlO_2^{-1}$, and the predominance of CN = 4 would increase, as predicted by Benoit and Ispas.[26]

By combining the descriptions of the liquid phase in the three side systems, we now arrive at the following formula for the whole system: $(Al^{+3}, Ca^{+2})_P(AlO_2^{-1}, O^{-2}, SiO_4^{-4}, SiO_2^0)_Q$. However, in order not to allow the $O^{-2}$ and $SiO_4^{-4}$ species to have a noticeable influence on the $SiO_2–Al_2O_3$ system, the Gibbs energy of the end members $(Al^{+3})_2(O^{-2})_3$ and $(Al^{+3})_4(SiO_4^{-4})_3$ will be assigned large positive values.

The model yields complicated thermodynamic expressions but, in practice, all calculations have been carried out automatically with some thermodynamic software package. The Gibbs energy of the liquid phase in the $CaO–Al_2O_3–SiO_2$ sytem is given by

$$G_m = \sum\sum y_i y_j^o G_{ij} + Q\sum y_k^o G_k + PRT\sum y_i \ln y_i + QRT\left(\sum y_j \ln y_j + \sum y_k \ln y_k\right) + {}^E G_m \quad (1)$$

where $i$ is a cation, $Al^{+3}$ or $Ca^{+2}$, and $j$ is an anion, $AlO_2^{-1}$, $O^{-2}$ or $SiO_4^{-4}$, and $k$ is a neutral, $SiO_2^0$. Electroneutrality is maintained by varying $P$ and $Q$ as

$$P = y_{AlO_2^{-1}} + 2y_{O^{-2}} + 4y_{SiO_4^{-4}},$$
$$Q = 3y_{Al^{+3}} + 2y_{Ca^{+2}} \quad (2)$$

The last term ${}^E G_m$ in Eq. (1) is the excess Gibbs energy that defines the interaction parameters as follows:

$$\begin{aligned}
{}^E G_m =& y_{Al^{+3}} y_{Ca^{+2}} y_{AlO_2^{-1}} {}^0L_{Al^{+3},Ca^{+2}:AlO_2^{-1}} \\
&+ y_{Al^{+3}} y_{AlO_2^{-1}} y_{SiO_2^0} ({}^0L_{Al^{+3}:AlO_2^{-1},SiO_2^0} + {}^1L_{Al^{+3}:AlO_2^{-1},SiO_2^0}(y_{AlO_2^{-1}} - y_{SiO_2^0})) \\
&+ y_{Ca^{+2}} y_{AlO_2^{-1}} y_{O^{-2}} ({}^0L_{Ca^{+2}:AlO_2^{-1},O^{-2}} + {}^1L_{Ca^{+2}:AlO_2^{-1},O^{-2}}(y_{AlO_2^{-1}} - y_{O^{-2}})) \\
&+ y_{Ca^{+2}} y_{AlO_2^{-1}} y_{SiO_2^0} ({}^0L_{Ca^{+2}:AlO_2^{-1},SiO_2^0} + {}^1L_{Ca^{+2}:AlO_2^{-1},SiO_2^0}(y_{AlO_2^{-1}} - y_{SiO_2^0})) \\
&+ y_{Ca^{+2}} y_{O^{-2}} y_{SiO_2^0} ({}^0L_{Ca^{+2}:O^{-2},SiO_2^0} + {}^1L_{Ca^{+2}:O^{-2},SiO_2^0}(y_{O^{-2}} - y_{SiO_2^0}) \\
&+ {}^2L_{Ca^{+2}:O^{-2},SiO_2^0}(y_{O^{-2}} - y_{SiO_2^0})^2 + {}^3L_{Ca^{+2}:O^{-2},SiO_2^0}(y_{O^{-2}} - y_{SiO_2^0})^3) \\
&+ y_{Al^{+3}} y_{Ca^{+2}} y_{SiO_4^{-4}} y_{SiO_2^0} {}^0L_{Al^{+3}Ca^{+2}:SiO_4^{-4},SiO_2^0} \\
&+ y_{Ca^{+2}} y_{SiO_4^{-4}} y_{SiO_2^0} ({}^0L_{Ca^{+2}:SiO_4^{-4},SiO_2^0} + {}^1L_{Ca^{+2}:SiO_4^{-4},SiO_2^0}(y_{SiO_4^{-4}} - y_{SiO_2^0}) \\
&+ {}^2L_{Ca^{+2}:SiO_4^{-4},SiO_2^0}(y_{SiO_4^{-4}} - y_{SiO_2^0})^{+23}L_{Ca^{+2}:SiO_4^{-4},SiO_2^0}(y_{SiO_4^{-4}} - y_{SiO_2^0})^3) \\
&+ y_{Ca^{+2}} y_{AlO_2^{-1}} y_{SiO_4^{-4}} y_{SiO_2^0} (v_1 {}^0L_{Ca^{+2}:AlO_2^{-1},SiO_4^{-4},SiO_2^0} \\
&+ v_2 {}^1L_{Ca^{+2}:AlO_2^{-1},SiO_4^{-4},SiO_2^0} + v_3 {}^2L_{Ca^{+2}:AlO_2^{-1},SiO_4^{-4},SiO_2^0})
\end{aligned} \quad (3)$$

where ${}^iL$ $(i = 0,1,2,3)$ represents the binary interactions between the species within a sublattice and $v_i$ $(i = 1,2,3)$ represents ternary interactions.[2] They are defined as

$$v_1 = y_{AlO_2^{-1}} + f, v_2 = y_{SiO_4^{-4}} + f, v_3 = y_{SiO_2^0} + f$$
$$f = (1 - y_{AlO_2^{-1}} - y_{SiO_4^{-4}} - y_{SiO_2^0})/3 \quad (4)$$

All solid phases except for mullite will be described as stoichiometric phases. Their molar Gibbs energies are represented by

expressions of the following type:

$$^{\circ}G_m - H^{SER} = A + BT^{-1} + CT + DT\ln T + ET^2 + FT^{-2} \quad (5)$$

## III. Experimental Data

### (1) Solid Phases

There are four ternary compounds in this $CaO$–$Al_2O_3$–$SiO_2$ system, namely gehlenite ($Ca_2Al_2SiO_7$), anorthite ($CaAl_2Si_2O_8$), clinopyroxene ($CaAl_2SiO_6$), and grossular ($Ca_3Al_2Si_3O_{12}$). For gehlenite, the relative enthalpy ($H_T$–$H_{298}$) measured by Pankratz and Kelley,[28] heat capacity ($C_P$) at 25°C by Weller and Kelley,[29] and entropy ($S$) at 25°C by Hemingway and Robie[30] were used in the assessment. The enthalpy of formation at 25°C, $\Delta_f H_{298}$, was taken from the evaluation by Robinson *et al.*[31] For anorthite, $C_P$ and $S$ at 25°C were taken from King,[32] and $\Delta_f H_{970}$ from the measurement by Charlu *et al.*[33] The information on $H_T$–$H_{298}$ was taken from the evaluation by Robinson *et al.*[31] The other two compounds, clinopyroxene and grossular, are stable only at high pressure, and they were not assessed in the present work.

### (2) Liquid Phase

The isoactivity lines of $SiO_2$ in the liquid have been studied by many researchers. Kay and Taylor[34] measured $SiO_2$ activity at 1450°, 1500°, and 1550°C through the equilibrium CO pressure for the reaction $SiO_2 + 3C \rightarrow SiC + 2CO$. Later on, Rein and Chipman[35,36] measured the same quantity at 1550° and 1600°C by equilibration with Fe–Si–C alloys in CO gas. The activity of CaO at 1500°C was measured by Kalyanram *et al.*[37] by the equilibration between the CO–$CO_2$–$SO_2$ gas and CaO–$Al_2O_3$–$SiO_2$ slag. Choosing Sn as the solvent and studying the slag–metal equilibria, Zhang *et al.*[38] measured the activities of CaO at 1600°C. Direct experimental measurement of the activities of $Al_2O_3$ in the liquid is lacking. The stable miscibility gap of liquid phase in the CaO–$Al_2O_3$–$SiO_2$ system was investigated by Greig.[39]

### (3) Phase Diagram

The phase diagram constructed by Osborn and Muan[40] based on critically assessed data from several sources was used in the present assessment. The phase $12CaO \cdot 7Al_2O_3$ was not included in the present study, as it has been shown to be unstable in the anhydrous CaO–$Al_2O_3$ system.[41]

## IV. Optimization

It was first necessary to reassess the CaO–$Al_2O_3$ and $Al_2O_3$–$SiO_2$ systems with the new model, although rather satisfactory assessments were already available. These reassessments on binary systems have been reported elsewhere.[42,43] Assessment of the CaO–$Al_2O_3$–$SiO_2$ ternary system is presented in this paper. All the assessment work was carried out with the ordinary CALPHAD technique[44] using the PARROT optimization module in the Thermo-Calc software package.[45]

During the optimization, the properties of the ternary compounds, gehlenite and anorthite, were assessed first. Thereafter, the liquid phase was included. Particular attention was paid to the liquid miscibility gap at the $Al_2O_3$-poor side. Positive values of the ternary interaction parameter $L_{Ca^{+2}:AlO_2^{-1}, SiO_4^{-4}, SiO_2^0}$ could be used to depress the miscibility gap close to the $SiO_2$ corner, and the binary parameter $L_{Ca^{+2}:AlO_2^{-1}, SiO_4^{-4}, SiO_2^0}$ could be used to depress the miscibility gap further so that the gap experiences difficulties in crossing the $SiO_2$–$CaAl_2O_4$ pseudo-binary line extending from the CaO–$SiO_2$ binary system. Finally, the parameter $L_{Al^{+3}, Ca^{+2}:SiO_4^{-4}, SiO_2^0}$ helps to make the stable part of the miscibility gap as narrow as indicated by experiments.[39] As a final stage of optimization, all items of experimental information were entered with proper weights, and the parameters for all the ternary phases were adjusted to obtain a self-consistent thermodynamic data set.

## V. Results

The thermodynamic properties of ternary compounds assessed in the CaO–$Al_2O_3$–$SiO_2$ system are listed in Table I. For the sake of completeness of the dataset, compatible data for the two high-pressure compounds, grossular and clinopyroxene, which were excluded in the present assessment, have been inserted in this table directly from Wang *et al.*[13] Information on $H_T$–$H_{298.15}$ for anorthite and gehlenite fitted very well, and comparisons between other experimental and calculated thermochemical properties of anorthite and gehlenite are shown in Table II. The agreement was also excellent. A complete list of thermodynamic properties of liquid is given in Table III. With the present descriptions of solid and liquid phases, various phase diagrams and thermodynamic properties can be determined. The liquidus projection and isothermal sections at 100°C intervals are illustrated in Fig. 1, and the properties of the corresponding invariant points in this diagram are compared with experiments in Table IV. The phase diagram calculated from the present assessment is nearly identical to the experimental one by Osborn and Muan,[40] except for the exclusion of the phase $12CaO \cdot 7Al_2O_3$ in the present work. It can also be seen in Table IV that the calculated and measured properties agree well for the eutectic, peritectic, and saddle points. In general, the difference is within 25°C and 2.5 mass%. The maximum difference in temperature is 70°C, for the equilibrium between $\alpha$-$Ca_2SiO_4$, $C_3A_1$, and hatrurite, and 4.2 mass% of $Al_2O_3$, for the equilibrium between anorthite, corundum, and mullite. The $Al_2O_3$ content of the liquid in the three-phase equilibrium between cristobalite and two liquids does not exceed 3 mass%, which is illustrated in Figs. 1 and 2.

Figure 2(a) shows the calculated isothermal section at 1650°C, and Fig. 2(b) gives an enlargement of the liquid miscibility gap close to the $SiO_2$ corner. With increasing temperature, the boundary of the miscibility gap will shift toward the CaO–$SiO_2$ binary. The temperature of the consolute point in the binary is calculated as 1686°C. On the other hand, with decreasing temperature, the Cri.+Liq. phase field will extend to higher $Al_2O_3$ contents faster than the miscibility gap, and the latter will become metastable below 1617°C. It never reaches more than 3 mass% $Al_2O_3$. The isothermal section at 1500°C is given in Fig. 3, where the two ternary compounds, gehlenite and anorthite, are stable.

The activities of $Al_2O_3$, $SiO_2$, and CaO in the ternary liquid are demonstrated in Figs. 4–6. The data are referred to the corresponding stable pure solid oxides at a given temperature. Figure 4 shows the calculated isoactivity lines of $Al_2O_3$ at 1550°C. Figures 5(a) and (b) compare the calculated activities

**Table I. $^{\circ}G_m$–$H^{SER}$ of Ternary Intermediate Compounds (in SI Units per Mole of Formula Unit)**

| |
|---|
| Anorthite ($CaAl_2Si_2O_8$) |
| $-4305540 - 529432/T + 1413.72T - 235.588T\ln T$ |
| $-0.0409767T^2 + 27151000/T^2$ |
| Gehlenite ($Ca_2Al_2SiO_7$) |
| $-4063100 - 360217/T + 1474.10T - 246.782T\ln T$ |
| $-0.0228876T^2 + 284128000/T^2$ |
| †Grossular ($Ca_3Al_2Si_3O_{12}$) |
| $-1120472 + 5991953/T + 2824.046T - 447.5989T\ln T$ |
| $-0.02781037T^2$ |
| †Clinopyroxene ($CaAl_2SiO_6$) |
| $-492365.4 + 3261763/T + 1451.554T - 231.3148T\ln T$ |
| $-0.01210426T^2$ |

†Data of grossular and clinopyroxene taken from Wang *et al.*[13]

**Table II. Thermochemical Properties of Anorthite and Gehlenite (in SI Units per Mole of Formula Unit)**

| Phase | Property | This assessment | Experiment | Reference |
|---|---|---|---|---|
| Anorthite ($CaAl_2Si_2O_8$) | | | | |
| | $C_{P298}$ | 210.5 | 211.6 | King[32] |
| | $S_{298}$ | 203.1 | 202.5 | King[32] |
| | $\Delta_f H_{970}$ | −101227 | −100123 | Charlu *et al.*[33] |
| Gehlenite ($Ca_2Al_2SiO_7$) | | | | |
| | $C_{P298}$ | 204.2 | 204.6 | Weller and Kelley[29] |
| | $S_{298}$ | 209.8 | 209.8 | Hemingway and Robie[30] |
| | $\Delta_f H_{298}$ | −124085 | −125110 | Robinson *et al.*[31] |

of $SiO_2$ at 1550° and 1600°C with various measurements.[34–36] The numbers in the diagram give the activity values. The different axis variables should be noticed among these diagrams. The activities of CaO at 1600° and 1500°C are plotted in Fig. 6 and compared with the experiments.[37,38] In Fig. 6(a), the calculated isoactivity lines for 0.003 and 0.5 fall at lower CaO content than the measured lines by Zhang *et al.*,[38] but there is a reasonable agreement for isoactivity lines between 0.008 and 0.25. In Fig. 6(b), the fit is rather satisfactory for isoactivity lines for values higher than 0.007, but the calculated lines for 0.003 and 0.005 fall at higher CaO content compared with the experimental data from Kalyanram *et al.*[37] It appears that the calculated lines for CaO activities are a reasonable compromise between the two experimental studies.

More attention was paid to gehlenite and anorthite, the two ternary compounds. The liquidus properties and their pseudo-binary phase diagrams are given in Figs. 7–9. It can be seen that the agreement between the present calculation and the various measurements[40,46–48] is good.

## VI. Discussion

In the present work, the new species $AlO_2^{-1}$ was introduced to model the liquid phase in the $CaO–Al_2O_3–SiO_2$ system. The predicted stable miscibility gap of liquid at the $Al_2O_3$-poor side was consistent with the experiment.[39] It is interesting to examine how the miscibility gap develops at lower temperatures when it becomes metastable. According to our calculation, a stable miscibility gap in the $CaO–SiO_2$ binary system begins to develop at

**Table III. Thermodynamic Property of Liquid $(Al^{+3}, Ca^{+2})_P(AlO_2^{-1}, O^{-2}, SiO_4^{-4}, SiO_2)_Q$[†]**

| | |
|---|---|
| ${}^\circ G_{Al_2O_3} - H^{SER}$ | |
| $298.15 < T < 600.00$ | $-1607850.8+405.559491T-67.4804T \ln T-0.06747T^2+1.4205433\times10^{-5}T^3+938780T^{-1}$ |
| $600.00 < T < 1500.00$ | $-1625385.57+712.394972T-116.258T \ln T-0.0072257T^2+2.78532\times10^{-7}T^3+2120700T^{-1}$ |
| $1500.00 < T < 1912.00$ | $-1672662.69+1010.9932T-156.058T \ln T+0.00709105T^2-6.29402\times10^{-7}T^3+12366650T^{-1}$ |
| $1912.00 < T < 2327.00$ | $+29178041.6-168360.926T+21987.1791T \ln T-6.99552951T^2+4.10226192\times10^{-4}T^3-7.98843618\times10^9T^{-1}$ |
| $2327.00 < T < 4000.00$ | $-1757702.05+1344.84833T-192.464T \ln T$ |
| ${}^\circ G_{SiO_2} - H^{SER}$ | |
| $298.15 < T < 2980.00$ | $-923689.98+316.24766T-52.17T \ln T-0.012002T^2+6.78\times10^{-7}T^3+665550T^{-1}$ |
| $2980.00 < T < 4000.00$ | $-957614.21+580.01419T-87.428T \ln T$ |
| ${}^\circ G_{CaO} - H^{SER}$ | |
| $298.15 < T < 1830.00$ | $-585630.854+300.654841T-52.862T \ln T-1.5545\times10^{-4}T^2-1.89185\times10^{-7}T^3+489415T^{-1}$ |
| $1830.00 < T < 2880.00$ | $-793806.269+1510.9933T-212.686T \ln T+0.0549185T^2-3.789867\times10^{-6}T^3+51730500T^{-1}$ |
| $2880.00 < T < 3172.00$ | $-4191941.74+15458.9937T-1961.24T \ln T+0.4554355T^2-2.1019333\times10^{-5}T^3+1.291855\times10^9T^{-1}$ |
| $3172.00 < T < 6000.00$ | $-663523.922+573.648795T-84T \ln T$ |
| ${}^\circ G_{Al^{+3}:AlO_2^{-1}}$ | $2{}^\circ G_{Al_2O_3}$ |
| ${}^\circ G_{Ca^{+2}:AlO_2^{-1}}$ | ${}^\circ G_{Al_2O_3} + {}^\circ G_{CaO} - 104900$ |
| ${}^\circ G_{Al^{+3}:O^{-2}}$ | ${}^\circ G_{Al_2O_3} + 900000$ |
| ${}^\circ G_{Ca^{+2}:O^{-2}}$ | $2{}^\circ G_{CaO}$ |
| ${}^\circ G_{Al^{+3}:SiO_4^{-4}}$ | $2{}^\circ G_{Al_2O_3} + 3{}^\circ G_{SiO_2} + 300000$ |
| ${}^\circ G_{Ca^{+2}:SiO_4^{-4}}$ | $4{}^\circ G_{CaO} + 2{}^\circ G_{SiO_2} - 392874.98 + 0.739049T$ |
| ${}^0L_{Al^{+3}, Ca^{+2}: AlO_2^{-1}}$ | $-34100$ |
| ${}^0L_{Al^{+3}:AlO_2^{-1}, SiO_2^0}$ | 46900 |
| ${}^1L_{Al^{+3}:AlO_2^{-1}, SiO_2^0}$ | $-42000$ |
| ${}^0L_{Ca^{+2}: AlO_2^{-1}, O^{-2}}$ | $-188000+60.2T$ |
| ${}^1L_{Ca^{+2}: AlO_2^{-1}, O^{-2}}$ | 35800 |
| ${}^0L_{Ca^{+2}:AlO_2^{-1}, SiO_2^0}$ | $-157000+42.4T$ |
| ${}^1L_{Ca^{+2}:AlO_2^{-1}, SiO_2^0}$ | $-194000+76T$ |
| ${}^0L_{Ca^{+2}:AlO_2^{-1}, SiO_4^{-4}, SiO_2^0}$ | 121000 |
| ${}^1L_{Ca^{+2}:AlO_2^{-1}, SiO_4^{-4}, SiO_2^0}$ | 91000 |
| ${}^2L_{Ca^{+2}:AlO_2^{-1}, SiO_4^{-4}, SiO_2^0}$ | $-669000$ |
| ${}^0L_{Ca^{+2}:O^{-2}, SiO_2^0}$ | $-34.8213994T$ |
| ${}^1L_{Ca^{+2}:O^{-2}, SiO_2^0}$ | $-131148.943+55.8484556T$ |
| ${}^2L_{Ca^{+2}:O^{-2}, SiO_2^0}$ | $38208-14.3524231T$ |
| ${}^3L_{Ca^{+2}:O^{-2}, SiO_2^0}$ | $-41296$ |
| ${}^0L_{Al^{+3},Ca^{+2}:SiO_4^{-4},SiO_2^0}$ | $-608000$ |
| ${}^0L_{Ca^{+2}:SiO_4^{-4}, SiO_2^0}$ | ${}^0L_{Ca^{+2}:O^{-2}, SiO_2^0}$ |
| ${}^1L_{Ca^{+2}:SiO_4^{-4}, SiO_2^0}$ | ${}^1L_{Ca^{+2}:O^{-2}, SiO_2^0}$ |
| ${}^2L_{Ca^{+2}:SiO_4^{-4}, SiO_2^0}$ | ${}^2L_{Ca^{+2}:O^{-2}, SiO_2^0}$ |
| ${}^3L_{Ca^{+2}:SiO_4^{-4}, SiO_2^0}$ | ${}^3L_{Ca^{+2}:O^{-2}, SiO_2^0}$ |

[†]All parameter values are given in SI units.

**Table IV. Comparison of Calculated and Experimental Special Points Along the Liquidus Surface**

| | | Calculated value (measured value) | | |
|---|---|---|---|---|
| | | | Liquid composition mass% | |
| Type of point | Solid phases equilibrium with liquid | Temperature (°C) | $Al_2O_3$ | $SiO_2$ |
| Congruent melting | Ano | 1549 (1555) | | |
| | Geh | 1584 (1595) | | |
| Eutectic | $\alpha+C_1A_1+C_3A_1$ | | | |
| | $\alpha+C_1A_1+$"$C_{12}A_7$" | 1290 (1337) | 38.7 (41.8) | 8.7 (6.4) |
| | $Ano+C_1A_6+Geh$ | 1368 (1382) | 39.8 (39.4) | 31.0 (31.0) |
| | Ano+Geh+PsW | 1270 (1267) | 18.9 (20.0) | 42.8 (42.0) |
| | Ano+Mul+Tri | 1326 (1347) | 18.5 (20.0) | 73.4 (70.1) |
| | Ano+PsW+Tri | 1195 (1172) | 13.3 (14.8) | 62.4 (62.0) |
| | $C_1A_1+C_1A_2+Geh$ | 1474 (1502) | 50.6 (50.8) | 9.7 (9.7) |
| | Geh+PsW+Ran | 1308 (1312) | 12.9 (12.0) | 41.4 (40.7) |
| Peritectic | $\alpha+C_1A_1+Geh$ | 1370 (1382) | 38.0 (42.0) | 12.8 (9.7) |
| | $\alpha+C_3A_1+Hat$ | 1387 (1457) | 32.3 (33.0) | 10.3 (8.7) |
| | $\alpha+Geh+Ran$ | 1343 (1317) | 11.8 (11.9) | 40.1 (39.9) |
| | $Ano+C_1A_6+Cor$ | 1437 (1407) | 41.8 (39.7) | 31.8 (32.3) |
| | Ano+Cor+Mul | 1535 (1514) | 39.6 (36.7) | 43.6 (47.8) |
| | $C_1A_2+C_1A_6+Geh$ | 1497 (1472) | 48.7 (45.0) | 20.6 (24.0) |
| | $C_3A_1+Hat+Lim$ | 1406 (1472) | 32.0 (32.8) | 9.8 (7.5) |
| Saddle | $\alpha+Geh$ | 1525 (1547) | 23.2 (23.7) | 26.8 (26.7) |
| | Ano+Cor | 1544 (1549) | 41.4 (39.7) | 39.9 (41.1) |
| | Ano+Geh | 1370 (1387) | 36.9 (36.8) | 32.8 (33.0) |
| | Ano+PsW | 1292 (1309) | 16.2 (18.6) | 48.0 (47.3) |
| | Ano+Tri | 1332 (1370) | 17.5 (19.5) | 72.9 (70.0) |
| | $C_1A_2+Geh$ | 1546 (1554) | 50.3 (50.3) | 15.0 (15.0) |
| | Geh+PsW | 1308 (1320) | 12.9 (13.2) | 41.4 (41.1) |

$\alpha$, $\alpha$-$Ca_2SiO_4$; Ano, anothite; $C_1A_1$, $CaO \cdot Al_2O_3$; $C_1A_2$, $CaO \cdot 2Al_2O_3$; $C_1A_6$, $CaO \cdot 6Al_2O_3$; $C_3A_1$, $3CaO \cdot Al_2O_3$; "$C_{12}A_7$", $12CaO \cdot 7Al_2O_3$; Cor, corundum; Cri, cristobalite; Geh, gehlenitde; Hat, hatrurite; Lim, lime; Mul, mullite; PsW, pseudo-wollastanite; Ran, rankinite; Tri, tridymite.

1867°C. With the decrease of temperature, it is self-evident that the miscibility gap in the $CaO–Al_2O_3–SiO_2$ ternary extends toward the $Al_2O_3–SiO_2$ binary. At 1686°C, cristobalite appears in equilibrium with the two liquids. In the $Al_2O_3–SiO_2$ binary system, no stable miscibility gap exists. However, below 1383°C a metastable miscibility gap exists. Figure 10 shows the two calculated metastable miscibility gaps in the isothermal sections at 1027°, 1117°, 1227°, and 1427°C in $CaO–Al_2O_3–SiO_2$ ternary. At 1427°C, one metastable miscibility gap originates from the $CaO–SiO_2$ side. At 1227°C, two miscibility gaps, one originating from each binary side, extend toward each other. It was interesting to find that a "nose" appears at 1117°C around the consolute point of the miscibility gap from $CaO–SiO_2$ binary. This "nose" shows the attraction of the two miscibility gaps, and indicates a union at a lower temperature. At 1027°C, the two metastable miscibility gaps merge.

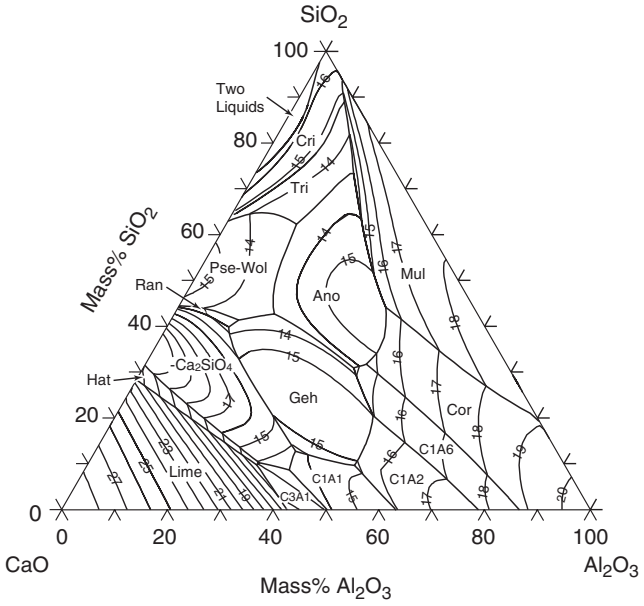


**Fig. 1.** Calculated phase diagram of the $CaO–Al_2O_3–SiO_2$ system. The thick curves represent three-phase equilibria with the liquid phase. The labeled areas show the liquidus surfaces for various solids. The thin curves represent the isothermal sections and the numbers stand for the temperatures with the unit as hundred Celsius. Ano, anorthite; C1A1, $CaO \cdot Al_2O_3$; C1A2, $CaO \cdot 2Al_2O_3$; C1A6, $CaO \cdot 6Al_2O_3$; C3A1,3 $CaO \cdot Al_2O_3$; Cor, corundum; Cri, cristobalite; Geh, gehlenite; Hat, Hatrurite; Mul, mullite; Pse-Wol, pseudo-wollastanite; Ran, rankinite; Tri, tridymite.

Figure 11 illustrates the calculated fractions of various species in the liquid phase at 85 mol% of $SiO_2$ and various temperatures. The $y$-axis represents the mole fraction of species with respect to the sum of species in both sublattices, including $Al^{+3}$, $Ca^{+2}$, $AlO_2^{-1}$, $O^{-2}$, $SiO_4^{-4}$, and $SiO_2^0$. The fraction of $O^{-2}$ is negligibly small at this high $SiO_2$ content. Fractions for the four species $Al^{+3}$, $Ca^{+2}$, $AlO_2^{-1}$, and $SiO_4^{-4}$ are plotted in the diagram and the balance is the dominant species $SiO_2^0$. The fraction of $Ca^{2+}$ is independent of temperature because $Ca^{+2}$ is the only species representing Ca with the present model. Besides the dominant species $SiO_2^0$, other two species $SiO_4^{-4}$ and $AlO_2^{-1}$ play important roles in liquid. In the $Al_2O_3$-poor part $SiO_4^{-4}$ becomes the second most dominant anion species, while in the $Al_2O_3$-rich part $AlO_2^{-1}$ does. This indicates that the miscibility gap extending from the $CaO–SiO_2$ side is caused by the repulsion of $SiO_2^0$ and $SiO_4^{-4}$, and the miscibility gap extending from the $Al_2O_3–SiO_2$ side is caused by the repulsion of $SiO_2^0$ and $AlO_2^{-1}$. At 1427°C, the fractions of species change smoothly. At 1227°C, there is a drastic decrease of the amounts of $SiO_4^{-4}$ and $Al^{+3}$ in the middle of the diagram, which falls on the $SiO_2–CaAl_2O_4$ section where all the Si and Al atoms could in principle enter a common network, represented here by the mixture of $SiO_2^0$ and $AlO_2^{-1}$. Then there would be no $SiO_4^{-4}$ or $Al^{+3}$ ions

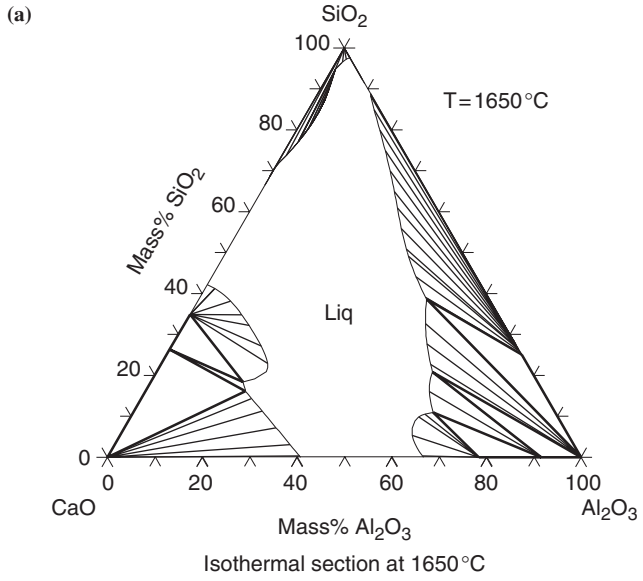


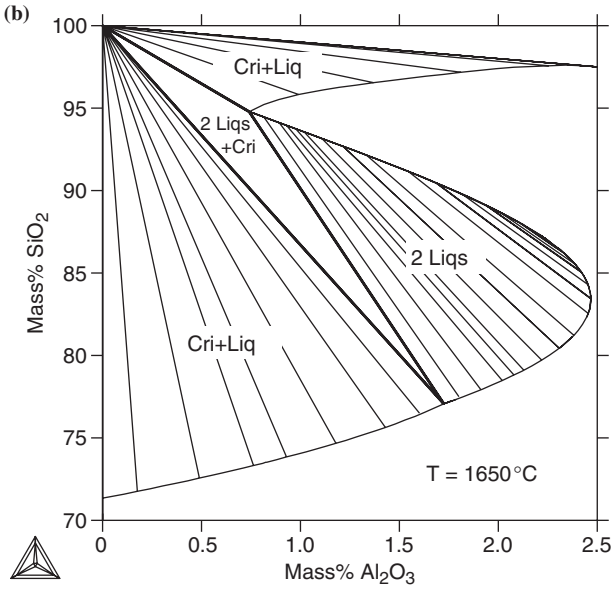


**Fig. 2.** Calculated extension of the liquid phase at 1650°C. The thick straight lines show the three-phase equilibrium fields. Liquid in the center of this diagram equilibrates with various solid phases. The tie lines are represented by thin straight lines. (a) Isothermal section at 1650°C. (b) Magnification of the $SiO_2$-rich part.

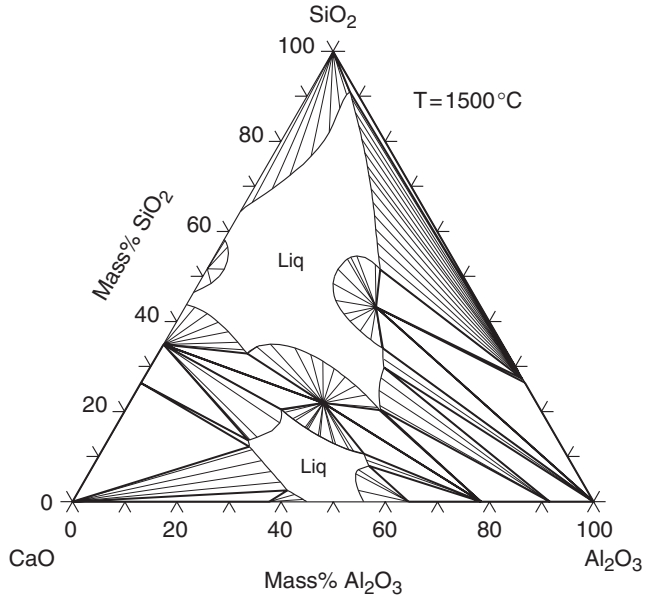


**Fig. 3.** Calculated isothermal section at 1500°C.

left. According to Fig. 11, this is predicted to occur at low temperatures. It is interesting to note from Fig. 10 that the extension of the miscibility gap from the CaO–$SiO_2$ side into the ternary system seems to be halted at the $SiO_2$–$CaAl_2O_4$ section, i.e., in the middle of the system. At first, it does not seem to help to decrease the temperature below 1227°C, and Fig. 11 now indicates that this is caused by the amount of $SiO_4^{-4}$ decreasing to very low values there. It may thus seem natural that the demixing tendency, caused by the repulsion between $SiO_2^0$ and $SiO_4^{-4}$, should not be able to extend beyond the $SiO_2$–$CaAl_2O_4$ section. It may be concluded that the small "nose" that is appearing beyond the $SiO_2$–$CaAl_2O_4$ section at 1117°C is primarily caused by the repulsion between $SiO_2^0$ and $AlO_2^{-1}$.

The present assessment has given a reasonable description of the experimental information, and the introduction of the $AlO_2^{-1}$ species has played an important part. This result gives some support to the belief that CN = 4 is predominating at high $Al_2O_3$ contents. However, this should not be taken as an indication that $Al^{+3}$ is less stable than $AlO_2^{-1}$ close to the CaO corner, which is formally predicted by the model because of the high value of $G_{Al^{+3}:O^{-2}}$. This value was chosen in order to suppress the $O^{-2}$ species on the $Al_2O_3$–$SiO_2$ side. Unintentionally, this parameter will also suppress the $Al^{+3}$ species close to the CaO corner where the amount of $O^{-2}$ is high. It should again be emphasized that the mixture of $O^{-2}$ and $AlO_2^{-1}$ on the anion sub-lattice was primarily intended to mimic the gradual fragmentation of the tetrahedral $AlO_2^{-1}$ network as the amount of O relative to Al is increased on the CaO-rich side of $CaAl_2O_4$ in the CaO–$Al_2O_3$ system. However, because of the low stability of $AlO_4^{-5}$, relative to $SiO_4^{-4}$, this process could also include dissociation of that $AlO_4^{-5}$ and the formation of $Al^{+3}$. In order to make the model yield reasonable amounts of $Al^{+3}$, it is necessary to change the method of preventing $O^{-2}$ to appear on the $Al_2O_3$–$SiO_2$ side. One possibility would be to introduce the interaction parameter $L_{Al^{+3}:O^{-2},AlO_2^{-1}}$ instead of $G_{Al^{+3}:O^{-2}}$.

In the present model, the new species $AlO_2^{-1}$ was introduced to mimic the tendency of Al to have a coordination number of

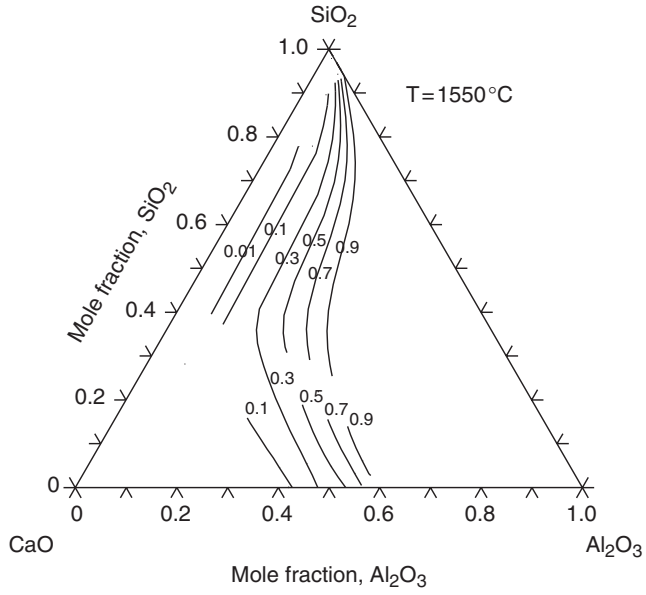


**Fig. 4.** Calculated isoactivity lines of $Al_2O_3$ in the field of stable liquid at 1550°C.

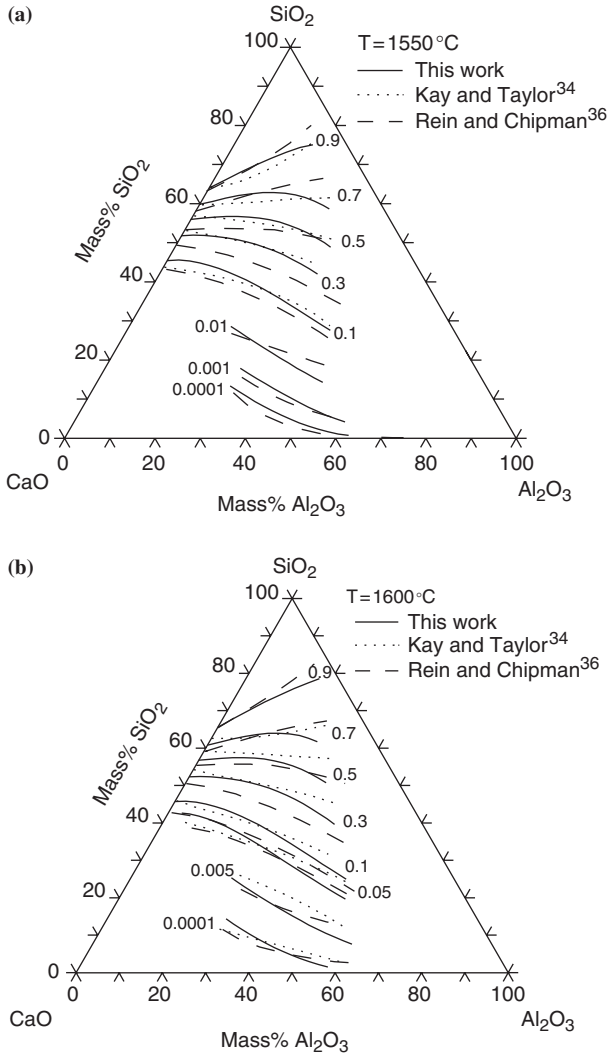


**Fig. 5.** Calculated and measured isoactivity lines of $SiO_2$ in stable liquid at various temperatures.

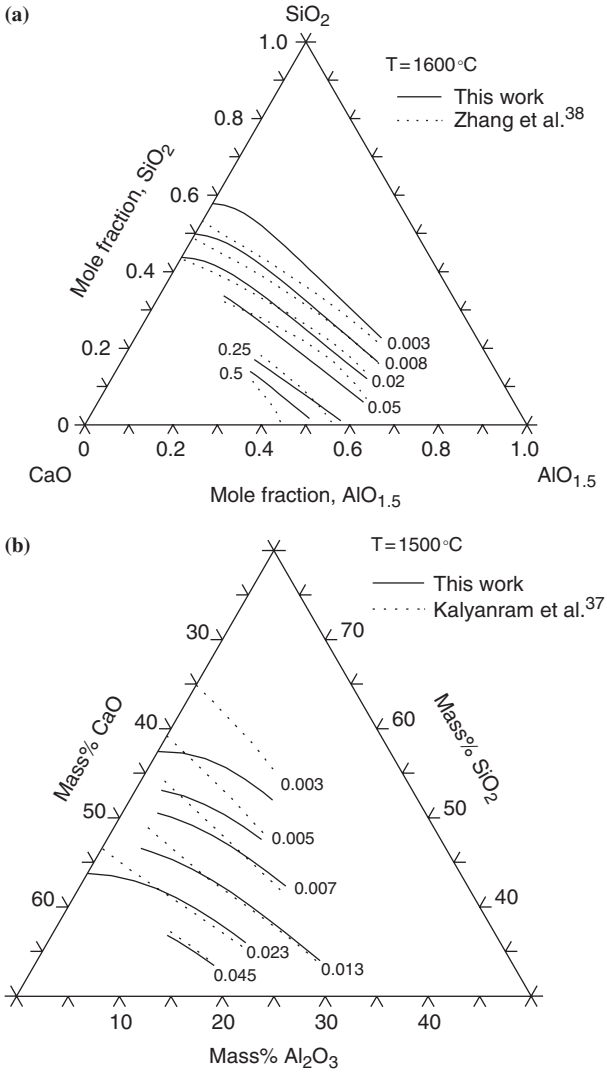


**Fig. 6.** Calculated and measured isoactivity lines of CaO in stable liquid.

CN = 4 and take part in the formation of a large network of Si and Al joined by bridging O atoms. As proposed by Kozakevitch,[22] viscosities of alumino-slags may be related to how perfect this network is. There have been some attempts to relate information on viscosity to the structure of the melt, e.g. by Zhang and Jahanshahi[49] and more recently by Nakamoto *et al.*[50] However, a very simple approach will now be tested by comparing lines of constant viscosity with the calculated site fractions of $SiO_2^0$ and $AlO_2^{-1}$, which represent the tendency to form a network. Comparison will be made with viscosity data at 1900°C from Kozakevitch.[22] Figure 12 has been drawn from his experimental points and is similar to the diagrams previously published by Richardson[23] and Mysen.[21] Figure 13 shows curves for constant site fractions of $SiO_2^0$, and they do not compare well with Fig. 12. Evidently, one should not neglect the effect of $AlO_2^{-1}$. In Fig. 14, the effect of each $AlO_2^{-1}$ is supposed to be the same as of each $SiO_2^0$. Comparison with Fig. 12 indicates that this is a severe overestimation of the effect of $AlO_2^{-1}$. In Fig. 15 the effect of $AlO_2^{-1}$ was assumed to be half of the effect of $SiO_2^0$ and the comparison with Fig. 12 is encouraging. The weaker effect of $AlO_2^{-1}$ may easily be explained by the Al–O bonds being weaker than Si–O bonds. This result may thus be taken as further support for the introduction of the $AlO_2^{-1}$ species into the model.

From a technical point of view, it is important to know or estimate the ability of a slag to purify iron melts from non-metallic impurities like S and P. This property is expressed directly by the sulfur and phosphorus capacities of the slag, which can be

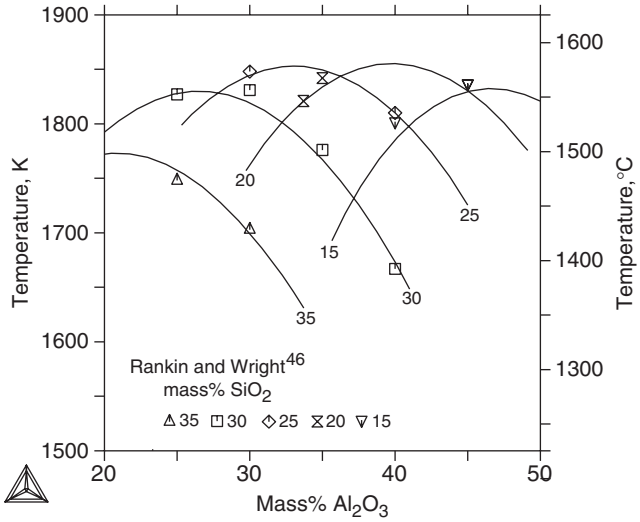


**Fig. 7.** Gehlenite liquidus within various isoplethal sections at constant $SiO_2$ contents. Symbols represent the experimental data by Rankin and Wright[46]; curves are calculated by the present assessment. The ends of the lines reflect the limited extension of stable liquid.

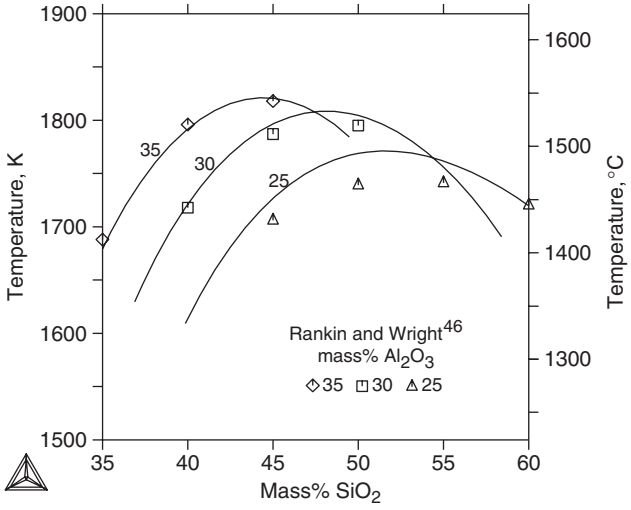


**Fig. 8.** Anorthite liquidus within various isoplethal sections at constant $Al_2O_3$ content. Symbols represent the experimental data by Rankin and Wright[46]; curves are calculated using the present assessment. The ends of the lines reflect the limited extension of stable liquid.

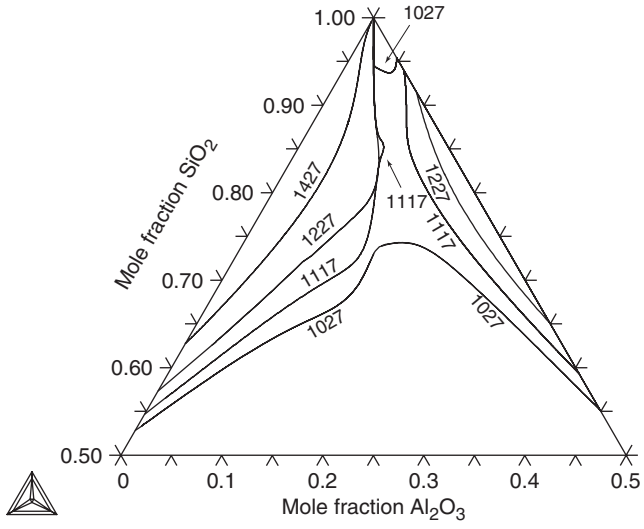


**Fig. 10.** Calculated metastable miscibility gaps in the isothermal sections at 1027°, 1117°, 1227°, and 1427°C.

measured experimentally. However, it is also of considerable interest to be able to predict this property. From a thermodynamic slag model, it should be possible to calculate such capacities directly from the composition of the slag through the activity coefficients. However, available models may not be accurate enough to yield reliable predictions. Several simpler methods are based on the concept of "basicity." Many different ways of calculating this property from the composition without using any model have been proposed.[51] One of the methods is based on the activity of CaO,[52] which may be easier to measure than the activity coefficient of S or P.

The relevance of the CaO activity for the ability to absorb S and P can be explained as follows; the explanation is based on the relation between the activity coefficient of $P_2O_5$ and the activity of CaO. When relating the activity of $P_2O_5$ to that of P, one has to define the activity of O, which, in principle, could be supplied by the iron melt or the atmosphere but in practice mainly from the slag if it contains elements like Fe and Mn with variable valence. It will be assumed that P is present in the slag as $PO_4^{-3}$ species. One would then have the following relation between chemical potentials (μ):

$$\mu_{P_2O_5} = 2\mu_{PO_4^{-3}} - 3\mu_{O^{-2}} = \mu_{Ca_3P_2O_8} - 3\mu_{CaO} \quad (6)$$

$$RT\ln\gamma_{P_2O_5} = \mu_{Ca_3P_2O_8} - 3\mu_{CaO} - RT\ln x_{P_2O_5} \quad (7)$$

It is seen that in order to decrease the activity coefficient of $P_2O_5$, $\gamma_{P_2O_5}$, and thus increase the ability of the slag to absorb P, one should increase $\mu_{CaO}$ and that quantity could be used to represent the basicity of the slag if the quantity $\mu_{Ca_3P_2O_8} RT \ln x_{P_2O_5}$ is sufficiently independent of the composition of the slag. This is thus the assumption behind the use of the activity of CaO. If the corresponding quantity for S is also independent of

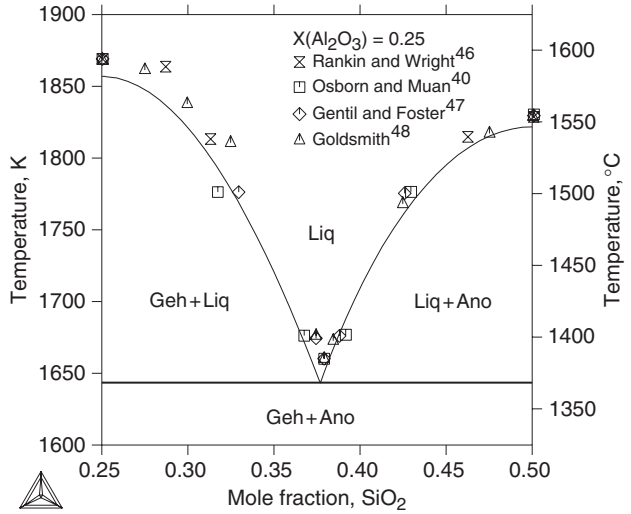


**Fig. 9.** Isoplethal through the gehlenite–anorthite pseudo-binary system. The $Al_2O_3$ content is constant at $X(Al_2O_3) = 0.25$ as the compositions are in mole fraction of the components $CaO–Al_2O_3–SiO_2$. Curves are calculated using the present assessment and symbols represent the experimental data from various sources.[40,46-48]

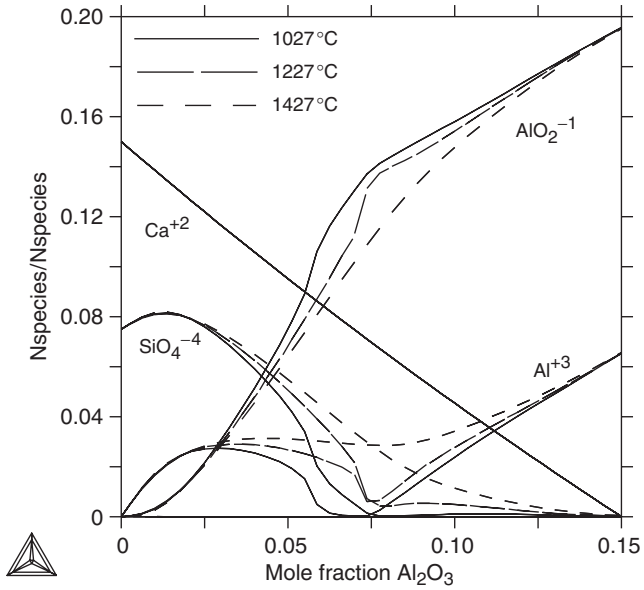


**Fig. 11.** Calculated fractions of various species in the liquid phase at 85 mol% of $SiO_2$ and various temperatures. The *Y*-axis represents the fraction of species with respect to total amount of species in both sublattices, including $Al^{+3}$, $Ca^{+2}$, $AlO_2^{-1}$, $O^{-2}$, $SiO_4^{-4}$, and $SiO_2^0$ according to our model. The fraction of $O^{-2}$ is very small and it is negligible in this case. Fractions of the four species $Al^{+3}$, $Ca^{+2}$, $AlO_2^{-1}$, and $SiO_4^{-4}$ are plotted in the figure and the balance is the dominant species $SiO_2^0$.

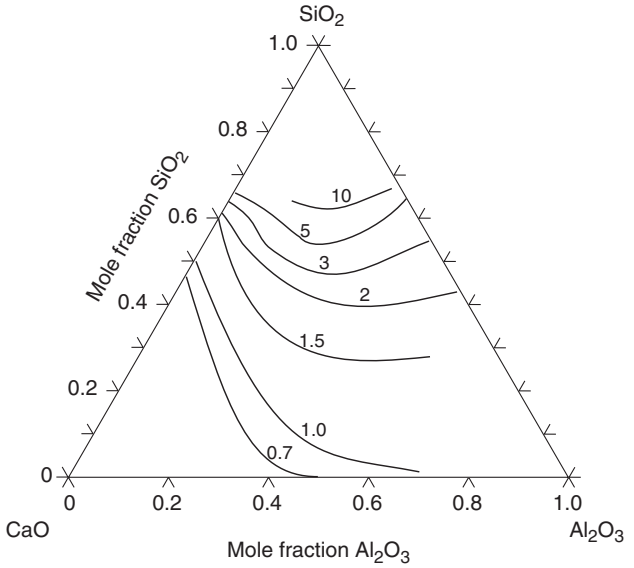


**Fig. 12.** Viscosities in poise for $CaO–Al_2O_3–SiO_2$ liquid at 1900°C (after Kozakevitch[22]).

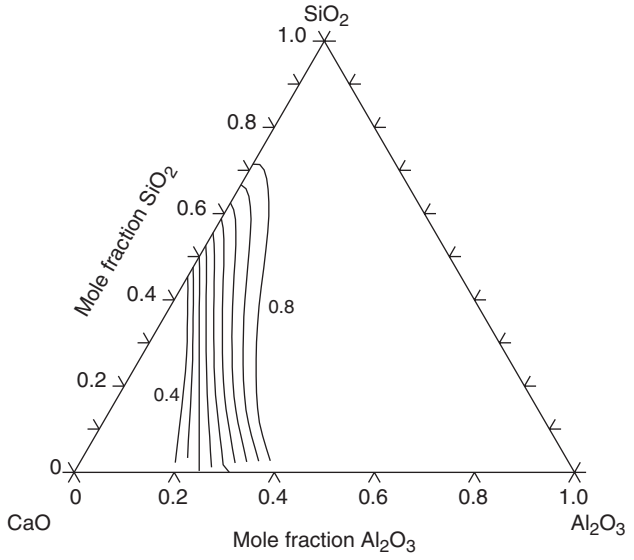


**Fig. 14.** Calculated iso-concentration lines for the amount of $y_{SiO_2^0} + y_{AlO_2^{-1}}$, between 0.4 and 0.8, with a 0.05 interval at 1900°C.

the composition of the slag, it would be justified to use the same basicity for S.

In order to extend this definition of basicity to slags containing other metals it would be necessary to add the chemical potentials of all the metals and with weights adjusted to their different abilities to decrease the activity coefficient of $P_2O_5$. In an attempt to make that summation unnecessary, one could look at the site fraction of the $O^{-2}$ species. This approach could only be justified by first examining whether this site fraction has the same effect on the ability to remove P or S independent of what metals are present in the slag. As a preliminary study, it was now examined how well the site fraction $y_{O}^{-2}$ follows $a_{CaO}$ in the $CaO–Al_2O_3–SiO_2$ system. Lines for a series of those two quantities were thus calculated from the present model, and have been plotted in Figs. 16 and 17. There is an encouraging similarity, and it may be interesting to continue this study by examining which of these two actually describes the purification power of the slag best.

## VII. Summary

Based on previous assessments of the three side systems, the thermodynamic properties and phase equilibria of the $CaO–Al_2O_3–SiO_2$ system have been assessed. A liquid model was applied including a new species $AlO_2^{-1}$ for the purpose of mimicking the tendency of $Al_2O_3$ to enter into the $SiO_2$ network. The assessment was successful and, in particular, it was possible to describe the reluctance of the liquid miscibility gap on the $CaO–SiO_2$ side to extend far into the ternary system. This has been surprising because there a similar miscibility gap exists on the $Al_2O_3–SiO_2$ system.

The calculated fraction of $AlO_2^{-1}$ seems to have an important effect on the viscosity, which is to be expected if $AlO_2^{-1}$ actually models the introduction of Al into the $SiO_2$ network.

The so-called sulfur and phosphorus capacities of slags are discussed in thermodynamic terms and the basis for approximating them with the CaO activity is emphasized. The alternative to use the fraction of $O^{-2}$, which can be calculated

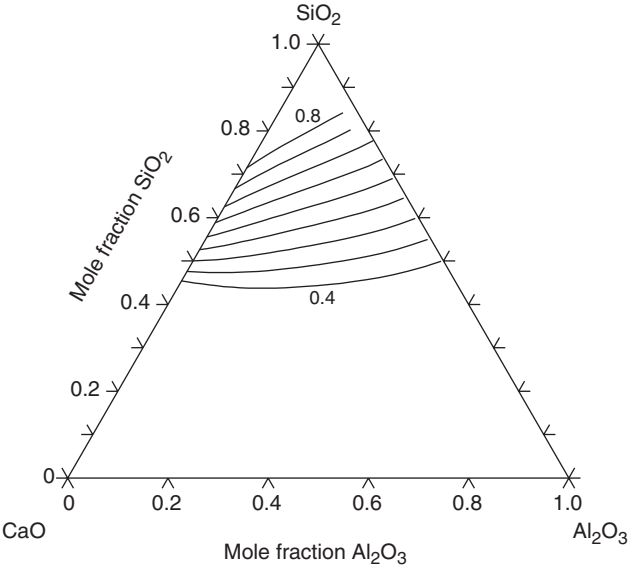


**Fig. 13.** Calculated iso-concentration lines for $y_{SiO_2^0}$ between 0.4 and 0.8, with a 0.05 interval at 1900°C.

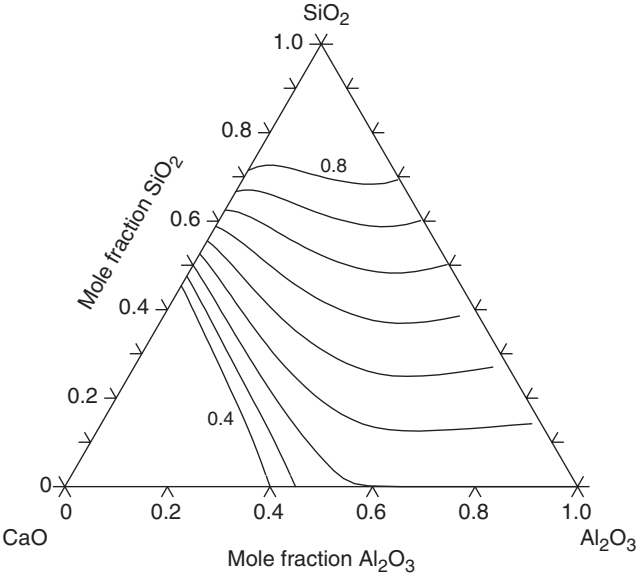


**Fig. 15.** Calculated iso-concentration lines for the amount of $y_{SiO_2^0} + 0.5 \times y_{AlO_2^{-1}}$, between 0.4 and 0.8, with a 0.05 interval at 1900°C.

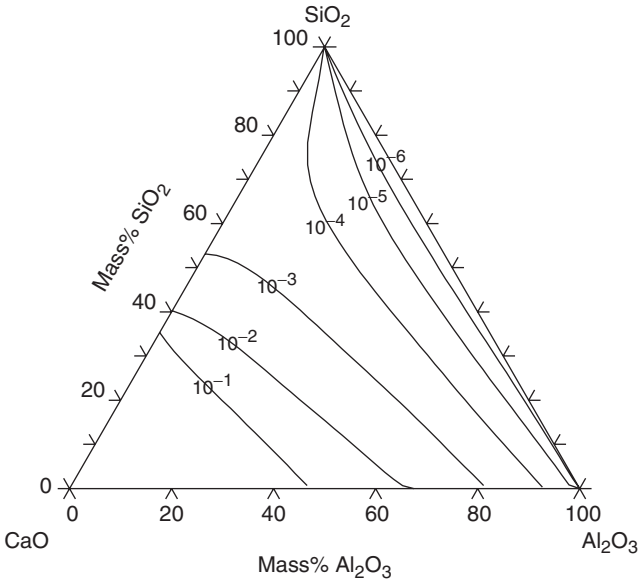


**Fig. 16.** Calculated iso-activity contours of CaO referred to the liquid phase at 1600°C.

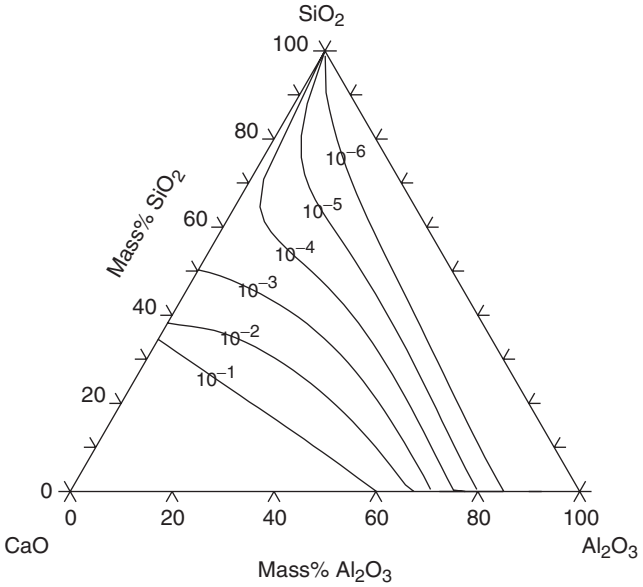


**Fig. 17.** Calculated iso-site-fraction contours of $O^{-2}$ in the CaO–$Al_2O_3$–$SiO_2$ liquid at 1600°C.

from the model after the slag system has been assessed, is also discussed.

## References


[1]M. Hillert, B. Jansson, B. Sundman, and J. Ågren, "A Two-Sublattice Model for Molten Solutions with Different Tendency for Ionization," *Metall. Trans.*, **16A**, 261–6 (1985).

[2]B. Sundman, "Modification of the Two-Sublattice Model for Liquids," *CALPHAD*, **15** [2] 109–19 (1991).

[3]A. D. Pelton and M. Blander, "Thermodynamic Analysis of Ordered Liquid Solutions by a Modified Quasi-Chemical Approach—Application to Silicate Slags," *Metall. Trans. B*, **17** [4] 805–1 (1986).

[4]G. Eriksson, P. Wu, M. Blander, and A. D. Pelton, "Critical Evaluation and Optimization of the Thermodynamic Properties and Phase Diagrams of the MnO–$SiO_2$ and CaO–$SiO_2$ Systems," *Canad. Metall. Quart.*, **33** [1] 13–21 (1994).

[5]M. Hillert, B. Sundman, and X. Z. Wang, "An Assessment of the CaO–$SiO_2$ System," *Metall. Trans. B*, **21** [2] 303–12 (1990).

[6]M. Hillert, B. Sundman, X. Z. Wang, and T. Barry, "A Reevalution of the Rankinite Phase in the CaO–$SiO_2$ System," *CALPHAD*, **15** [1] 53–8 (1991).

[7]L. Kaufman, "Calculation of Quasibinary and Quasiternary Oxide Systems 2," *CALPHAD*, **3** [1] 27–44 (1979).

[8]P. Dörner, L. J. Gauckler, H. Krieg, H. L. Lukas, G. Petzow, and J. Weiss, "Calculation and Representation of Multicomponent Systems," *CALPHAD*, **3** [4] 241–57 (1979).

[9]R. A. Howald and I. Eliezer, "Thermodynamic Properties of Mullite," *J. Phys. Chem.*, **82** [20] 2199–204 (1978).

[10]G. Eriksson and A. D. Pelton, "Critical Evaluation and Optimization of the Thermodynamic Properties and Phase Diagrams of the CaO–$Al_2O_3$, $Al_2O_3$–$SiO_2$ and CaO–$Al_2O_3$–$SiO_2$System," *Metall. Trans. B*, **24** [5] 807–16 (1993).

[11]M. Hillert, B. Sundman, and X. Wang, *A Thermodynamic Evaluation of the $Al_2O_3$–$SiO_2$ System*. KTH, Stockholm, 1989 TRITA-MAC-402.

[12]B. Hallstedt, "Assessment of the CaO–$Al_2O_3$ System," *J. Am. Ceram. Soc.*, **73** [1] 15–23 (1990).

[13]X. Wang, M. Hillert, and B. Sundman, "A Thermodynamic Evaluation of the CaO–$Al_2O_3$–$SiO_2$ System"; TRITA-MAC-407, KTH, Stockholm, 1989.

[14]M. L. Kapoor and G. M. Frohberg, *Proceedings of the Symposium on "Chemical Metallurgy of Iron and Steel,"* Sheffield, 1971.

[15]H. Gaye and J. Welfringer, "Using a Thermodynamic Model of Slags for Describing Mettalurgical Reactions"; pp. 357–75 in *Proceedings of the 2nd International Symposium on Metallurgical Slags and Fluxes, Lake Tahoe, TMS-AIME*, Edited by H. A. Fine and D. R. Gaskell Warrendale, PA, 1984, Metall. Soc. AIME, New York, 1984.

[16]J. M. Larrain and H. H. Kellogg, "Use of Chemical Species for Correlation of Solution Properties"; pp. 11–16, in *Calculation of Phase Diagrams and Thermochemistry of Alloy Phases*, Edited by Y. A. Chaug and J. J. Smith. Met. Soc. AIME, Warrendale, PA, 1979.

[17]J. W. Hastie, W. S. Horton, E. R. Plante, and D. W. Bonnell, "Thermodynamic Models of Alkali Vapor Transport in Silicate Systems," *High Temp.-High Pressures*, **14**, 669–79 (1982).

[18]B. Björkman, "An Assessment of the System Fe–O–$SiO_2$ Using a Structure Based Model for the Liquid Silicate," *CALPHAD*, **9** [3] 271–82 (1985).

[19]M. Hoch, "Application of the Hoch Arpshofen Model to the $SiO_2$–CaO–MgO–$Al_2O_3$ System," *CALPHAD*, **12** [1] 45–58 (1988).

[20]R. G. Berman and T. H. Brown, "A Thermodynamic Model for Multicomponent Melts, with Application to the System CaO–$Al_2O_3$–$SiO_2$," *Geochim. Cosmochim. Acta*, **48** [4] 661–78 (1984).

[21]B. O. Mysen, *Structure and Properties of Silicate Melts*. Elsevier, Amsterdam, 1988.

[22]P. Kozakevitch, "Viscosite et elements structuraux des aluminosilicates fondues: laitiers entre 1600 et 2100 C (in French)," *Rev. Metall.*, **57**, 148–60 (1960).

[23]F. D. Richardson, *Physical Chemistry of Melts in Metallurgy*, Vol. 1. Academic press, London, 1974.

[24]G. Gutierrez, A. B. Belonoshko, R. Ahuja, and B. Johansson, "Structural Properties of Liquid $Al_2O_3$: A Molecular Dynamics Study," *Phys. Rev. E*, **61**, 2723–9 (2000).

[25]D. K. Belashchenko and L. V. Skvortsov, "Molecular Dynamics Study of CaO–$Al_2O_3$ Melts," *Inorg. Mater.*, **37**, 476–81 (2001).

[26]M. Benoit and S. Ispas, "Structural Properties of Molten Silicates from ab initio Molecular-Dynamics Simulations: Comparison Between CaO–$Al_2O_3$–$SiO_2$ and $SiO_2$," *Phys. Rev. B*, **64**, 224205 (2001).

[27]G. Gruener, P. Odier, D. D. Meneses, P. Florian, and P. Richet, "Bulk and Local Dynamics in Glass-Forming Liquids: A Viscosity, Electrical Conductivity and NMR Study of Aluminosilicate Melts," *Phys. Rev. B.*, **64** [2] Art. 024206 (2001).

[28]L. B. Pankratz and K. K. Kelley, "High-Temperature Heat Contents and Entropies of Akermanite, Cordierite, Gehlenite and Merwinite"; U.S. Bureau of Mines, RI, 6555, 1964..

[29]W. W. Weller and K. K. Kelley, "Low Temperature Heat Capacities and Entropies at 298.15 K of Akermanite, Cordierite, Gehlenite and Merwinite"; U.S. Bureau of Mines, RI, 6343, 1963..

[30]B. S. Hemingway and R. A. Robie, "Enthalpies of Formation of Low Albite ($NaAlSi_3O_8$), Gibbsite($Al(OH)_3$), and $NaAlO_2$-Revised Values for $\Delta H_f^{298}$ and $\Delta G_f^{298}$ of Some Aluminosilicate Minerals," *J. Res. U.S. Geol. Surv.*, **5** [4] 413–29 (1977).

[31]G. R. Robinson Jr., J. L. Hass Jr., C. M. Schafer, and H. T. Haselton Jr., "Thermodynamic and Thermophysical Properties of Mineral Components of Basalts"; in *Physical Properties Data for Basalt*, Edited by L. H. Gevantman. Bureau of Standards, Washington, DC, 1982.

[32]E. G. King, "Low Temperature Heat Capacities and Entropies at 298.15 K of some Crystalline Silicates Containing Calcium," *J. Am. Chem. Soc.*, **79**, 5437–8 (1957).

[33]T. V. Charlu, R. C. Newton, and O. J. Kleppa, "Enthalpy of Formation of Some Lime Silicates by High-Temperature Solution Calorimetry, with Discussion of High-Pressure Phase Equilibia," *Geochim. Cosmochim. Acta*, **42** [4] 367–75 (1978).

[34]D. A. R. Kay and J. Taylor, "Activities of Silica in the Lime+Alumina+Silica System," *Trans. Faraday Soc.*, **56**, 1372–84 (1960).

[35]R. H. Rein and J. Chipman, "The Distribution of Silicon Between Fe–Si–C Alloys and $SiO_2$–CaO–MgO–$Al_2O_3$ Slags," *Trans. Metall. Soc. AIME*, **227**, 1193–203 (1963).

[36]R. H. Rein and J. Chipman, "Activities in the Liquid Solution $SiO_2$–CaO–MgO–$Al_2O_3$ at 1600°C," *Trans. Metall. Soc. AIME*, **233** [2] 415–25 (1965).

[37]M. R. Kalyanram, T. G. Macfarlane, and H. B. Bell, "The Activity of Calcium Oxide in Slags in the Systems CaO–MgO–$SiO_2$, CaO–$Al_2O_3$–$SiO_2$, and CaO–MgO–$Al_2O_3$–$SiO_2$ at 1500°C," *J. Iron Steel Inst. Lond.*, **195**, 58–64 (1960).

[38]Z. Zhang, J. Zhou, Y. Zou, and Y. Tian, "Activity of CaO in Liquid CaO–$SiO_2$–$Al_2O_3$ System," *Acta Metall. Sinica*, **22** [3] A256–64 (1986) (in Chinese).

[39]J. W. Greig, "Immiscibility in Silicate Melts," *Am. J. Sci.*, **13** [73, 5th Series] 1–154.

[40]E. F. Osborn and A. Muan, *Phase Equilibrium Diagrams of Oxide Systems, Plate 1. The System CaO–$Al_2O_3$–$SiO_2$.* American Ceramic Society and Edward Orton, Ir., Ceramic Foundation, Columbus, OH, 1960.
[41]R. W. Nurse, J. H. Welch, and A. J. Majumdar, "The $12CaO \cdot 7Al_2O_3$ Phase in the CaO–$Al_2O_3$ System," *Trans. Br. Ceram. Soc.*, **64**, 323–32 (1965).
[42]H. H. Mao, M. Selleby, and B. Sundman, "Phase Equilibria and Thermodynamics in the $Al_2O_3$–$SiO_2$ System—Modelling of Mullite and Liquid," *J. Am. Ceram. Soc.*, **88**, 2544–51 (2005).
[43]H. H. Mao, M. Selleby, and B. Sundman, "A Reevalution of the Liquid Phase in the CaO–$Al_2O_3$ and MgO–$Al_2O_3$ System," *CALPHAD*, **28**, 307–12 (2004).
[44]N. Saunders and A. P. Miodownik, *Calphad (Calculation of the Phase Diagram): A Comprehensive Guide*. Pergamon, Oxford, 1998.
[45]J.-O. Andersson, T. Helander, L. Höglund, P. Shi, and B. Sundman, "Thermo-Calc & DICTRA, Computational Tools for Materials Science," *CALPHAD*, **26**, 273–312 (2002).
[46]G. A. Rankin and F. E. Wright, "The Ternary System of CaO–$Al_2O_3$–$SiO_2$," *Am. J. Sci.*, **39**, 1–79 (1915).
[47]A. L. Gentile and W. R. Foster, "Calcium Hexaluminate and its Stability Relations in the System CaO–$Al_2O_3$–$SiO_2$," *J. Am. Ceram. Soc.*, **46**, 74–6 (1963).
[48]J. R. Goldsmith, "The System $CaAl_2Si_2O_8$–$Ca_2Al_2SiO_7$–$NaAlSiO_4$," *J. Geol.*, **15**, 383–7 (1947).
[49]L. Zhang and S. Jahanshahi, "Review and Modeling of Viscosity of Silicate Melts," *Metall. Mater. Trans.*, **29B** [1] 177–86, 187–95 (1998).
[50]M. Nakamoto, J. Lee, and T. Tanaka, "A Model for Estimation of Viscosity of Molten Silicate Slag," *ISIJ International*, **45** [5] 651–6 (2005).
[51]Verein deutscher eisenhüttenleute, *Slag Atlas*, 2nd edition, Verlag Stahleisen M.B.H., Düsseldorf, 1995.
[52]D. R. Gaskell, "Optical Basicity and the Thermodynamic Properties of Slags," *Metall. Trans.*, **20B**, 113–8 (1989). □